

**AERODYNAMIC PERFORMANCE ANALYSIS OF THE HYPERSONIC  
AIRBREATHING VEHICLE JAPHAR**

Ph. Duveau, R. Hallard, Ph. Novelli (ONERA, Châtillon, France)  
and Th. Eggers (DLR, Braunschweig, Germany)

**Abstract**

In 1997, DLR and ONERA joined in a common project called JAPHAR (Joint Airbreathing Propulsion for Hypersonic Application Research). The main objective of this project is to develop and test at ground a dual mode ramjet engine (DMR) combining both subsonic and supersonic combustion regimes. The other objective is to define a methodology to establish the thrust-minus-drag balance of the DMR on an experimental vehicle to be flown between Mach number 4 and 8.

This paper presents an ongoing effort for the design of an integrated propulsive system for JAPHAR flight test vehicle. Forebody, inlet and nozzle aerodynamic studies are conducted in close connection with the system studies and require CFD analysis as well as wind tunnel experiments.

A forebody parametric study based on turbulent Navier-Stokes calculations was conducted at ONERA. The main results are given in the paper, demonstrating the advantage of DLR waverider forebody. In addition, this paper gives an overview of the inlet studies conducted so far at ONERA. An internal compression inlet was designed and tested in S3MA wind tunnel, between Mach 3 and 5.5. Navier-Stokes calculations are in progress to calibrate numerical codes and to provide combustion people with realistic entry flow field conditions. Lastly, a preliminary design of a SERN nozzle (Single Expansion Ramp Nozzle) relying on inviscid calculations is presented.

**Introduction**

At the end of the eighties, there was a renewal of activity in hypersonic airbreathing propulsion, illustrated by various programs such as NASP in the USA or SANGER in Germany. In France, PREPHA program [1], initiated in the early nineties, was aimed at the study of single and two-stage-to-orbit airbreathing vehicles with particular focus on scramjet technologies. The objective was to increase the knowledge in

materials, CFD, aerodynamics and energetic in order to prepare future hypersonic airbreathing propulsion applications.

In 1997, at the end of SANGER and PREPHA programs, DLR and ONERA decided to join their efforts in a common project called JAPHAR (Joint Airbreathing Propulsion for Hypersonic Application Research). This project focuses on dual mode ramjet engine (DMR) technology and has two objectives : firstly to develop and test at ground a DMR and secondly to define an appropriate methodology to establish the thrust-minus-drag balance of the DMR on an experimental vehicle to be flown between Mach number 4 and 8.

This paper gives an overview of the aerodynamic studies conducted in the frame of JAPHAR project to define an integrated propulsive system for a flight test vehicle. In a first step, aerodynamic component studies have been undertaken separately to start the system studies. A more integrated design process is in progress in order to provide the system studies with accurate data for the propulsion performance calculations.

A numerical parametric study of the forebody taking into account several parameters such as the nose bluntness and width, the longitudinal compression at the bottom side and the cross section shape was conducted at ONERA. An internal compression inlet has been investigated, both experimentally and numerically and used as a reference configuration for the vehicle comparisons. In addition, SERN type nozzles have been investigated numerically in order to define a satisfying geometry.

The first part of the paper recalls the design constraints of JAPHAR experimental vehicle. The second one gives detailed results obtained in the frame of the forebody parametric study. The last two sections describe the inlet and nozzle studies conducted so far.

### **JAPHAR : mission and design constraints**

The general approach of JAPHAR project is fully discussed in [2,3]. The main objective of this project is to demonstrate DMR acceleration capabilities between Mach 4 and 8 on a flight test vehicle (figure 1). Hence there is no particular operational requirement for such a vehicle, except to cover the entire flight domain and all combustion regimes. The design of the vehicle is however strongly influenced by the combustion chamber design and particularly by the fuel injection technology. Indeed, a major concern at the beginning of the project was to take into account a realistic fuel injection device, with struts instead of wall injection, because this device is quite mandatory in a large scale scramjet engine [4]. The combustion chamber designed in the frame of JAPHAR has indeed many struts levels for an efficient fuel injection and mixing in the air. At Mach 4, the engine works in subsonic regime, while the combustion process around Mach 6 is a combination of both subsonic and supersonic flows; at Mach 8, supersonic combustion is fully developed. The operation of the DMR combustion chamber relies on the thermal throat principle which allows, among others, the inlet and the nozzle to be operated with a fixed geometry.

The height of the engine is 100 mm at the inlet station, which leads to a 2.5 meter long engine. This design parameter influences the vehicle sizing to a great extent. Indeed, the inlet dimensions are readily deduced from the knowledge of the optimum contraction ratio allowing a fixed geometry inlet to be operated satisfactorily throughout the entire flight domain and the engine height. The main constraint is then to find a preliminary forebody shape ensuring that the front shock stays outside the inlet at Mach 8. Euler calculations were performed for this purpose, showing that the minimum forebody length was around 4.5 meters at Mach 8, incidence  $4^\circ$ . This leads to a vehicle length of 10 m, leaving 3 m for nozzle afterbody integration.

It was decided that no active cooling nor variable geometry should be accepted on a flight test vehicle. Then, an appropriate way to demonstrate DMR capabilities is to select a few combustion periods along a decelerating trajectory at constant dynamic pressure, from Mach 8 to Mach 4. This solution has the drawback to increase the initial boosting complexity, but, on the other hand, it alleviates the inlet constraints associated with self-starting at low Mach number.

At the beginning of the project, people from DLR and ONERA had different approaches concerning the

vehicle design. Indeed, DLR had a strong background in waverider design [5,6] whereas ONERA was more used to classical wing-body vehicles. It was then decided to compare two different vehicles during the first design iteration (figure 2).

### **Forebody studies**

#### **Preliminary remarks**

The forebody design is a key issue for an hypersonic airbreathing vehicle since it influences to a great extent the design of the vehicle itself as well as the global aerodynamic performance [6,7]. The forebody drag must be as small as possible whereas the lift to drag ratio has to be optimised. In addition, longitudinal stability aspects associated with the forebody must be taken into account at an early stage of the vehicle design.

The inlet performance are also strongly dependent on the forebody precompression effect [7]. As far as hypersonic airbreathing propulsion is concerned, the propulsive system must indeed be closely integrated to the airframe. In particular, the forebody is expected to act as an efficient compression system prior to the inlet. The forebody has to provide the inlet with a large mass flow associated with minimum pressure recovery losses, small distortions in flow angularity, Mach number and other flow parameters. In the mean time, the average Mach number at the inlet face has to be reduced as much as possible in order to minimise the inlet design constraints.

Forebody precompression of the airflow depends on a great number of parameters. First of all, the cross section shape of the forebody at the bottom side (flat, convex or concave) is expected to have a major influence on the flow field delivered to the inlet because of three dimensional effects. Another important feature is the nose design. The influence of nose bluntness and spatula effect (increase in nose width) on the inlet entry conditions and on the external aerodynamic performance has to be assessed. Another parameter to be considered is the lower wall slope in the vertical symmetry plane (straight or cambered profiles).

#### **Preliminary forebody design**

In 1998, ONERA and DLR started the forebody studies for the definition of the experimental vehicle. In a first step, Euler computations were performed in order to identify a satisfying shape for the vehicle forebody. The main constraint at this stage was to find design parameters which ensured that the detached front shock

staid outside the inlet. DLR designed a 4.2 meter long waverider forebody and ONERA designed a 4.7 meter long so-called reference forebody (figure 3). They greatly differ in nose bluntness (respectively 6 mm and 60 mm in nose radius) because at the beginning of JAPHAR project, ONERA had some doubts on whether metallic materials could withstand the thermal loads expected at Mach number 8. Their cross sections are also very different; while the cross section of ONERA's reference forebody is almost flat at the bottom side, the waverider is characterised by its strong curvature in spanwise direction. On the other hand, the lower surface slopes are identical ( $6^\circ$ ).

Turbulent Navier-Stokes calculations were performed to characterise the flow field around those two forebodies. The whole flight domain was covered in order to provide the system studies with realistic data for the propulsion performance calculations. The flow conditions and assumptions are given hereafter :

- Mach number = 4 / 6 / 8
- $Re / m = 9.56.10^6 / 6.26.10^6 / 4.58.10^6$ ,
- incidence  $0^\circ / +2^\circ / +4^\circ$ , sideslip angle =  $0^\circ$ ,
- dynamic pressure :  $q = 80$  kPa,
- adiabatic wall at Mach 4,  $T_w = 1000$  K at Mach 6 and  $T_w = 1200$  K at Mach 8,
- turbulent flow from the nose tip,
- perfect gas.

The wall boundary conditions are deduced from a DLR study, documented in [3], taking into account radiation effects. This preliminary study demonstrated in addition that real gas effects only led to small differences in shock position at Mach 8, which justified the perfect gas assumption.

The aerodynamic model based on ONERA reference forebody is given on figure 4. The stream tube area ratio (indicating the amount of mass flow captured by the inlet), the average Mach number and the pressure recovery in the entry plane of the inlet are plotted against free stream Mach number. The averaging through the inlet projected front area relies on a conservative approach. Namely, the equivalent one-dimensional flow field conserving the mass flow and the momentum and total enthalpy fluxes is determined. The average parameters of the flow field delivered to the

inlet are calculated in a plane normal to the lower wall, at station  $X = 4.2$  m. The projected front area of the inlet is  $A_1 = 0.32$  m<sup>2</sup> (800 mm in width by 400 mm in height).

Irrespective of trimming considerations, it is clearly favourable to fly at incidence since the mass flow is a growing function of the angle of attack at given Mach number. In addition, an increase in incidence leads to reduced Mach number in front of the inlet associated with higher pressure recovery, which is favourable to the inlet operation.

#### Forebody parametric study

Following this first set of calculations, a forebody parametric study, based on turbulent Navier-Stokes analysis, was conducted at ONERA to identify the influence of cross section shape, nose shape and windward longitudinal compression on the aerodynamic characteristics and propulsion efficiency of the forebody. The comparisons take into account the aerodynamic criteria listed below :

- forebody length required for inlet integration,
- inlet entry conditions and precompression effect,
- aerodynamic coefficients,
- centre of pressure location.

In addition, geometric aspects like the available volume for fuel and system integration have to be taken into account.

#### Description of the forebody shapes

Six forebody shapes derived from ONERA reference configuration were designed by changing only one parameter at a time or by combining two parameter changes. A seventh forebody taken from the American literature [8] was chosen for its original features and somewhat modified to meet JAPHAR requirements. The main features of this forebody (referred to as Hyper X in the following) are the very wide nose looking like a straight leading edge and the narrow flat lower surface of constant width. Shaded views of these forebodies can be seen on figure 5. Table 1 gives further details about the nose design and the main effects studied.  $R_{VRef}$  and  $R_{HRef}$  respectively denote the nose radius of the reference forebody in the vertical symmetry plane and in the horizontal plane.

FOREBODY	$R_V / R_{V REF}$	$R_H / R_{H REF}$	EFFECT
REF	1	1	
MOD1	1	2	nose width
MOD2	1	2/3	nose width
MOD3	1/2	1	nose bluntness
MOD4	1/2	2	nose width and bluntness
MOD5	1	1	convex cross section
MOD6	1	1	cambered windside
HyperX	1/6	$\gg 1$	sharp and wide nose
Waverider	1/10	$\ll 1$	sharp nose concave edges

Table 1 : forebody characteristics

Modified shapes 1 to 6 and Hyper X configuration are 6.5 meter long because the required length for inlet integration is unknown a priori and has to be assessed.

#### Numerical approach

In order to limit the amount of calculations, simulations were performed at Mach number 8, incidence  $+2^\circ$ , only. Mach 8 is indeed the worst case for inlet integration since the bow shock is closer to the bottom side of the forebody. Moreover, as the vehicle is flown along a constant dynamic pressure trajectory, the Reynolds number is lower at high speed; hence thicker boundary layers are expected at Mach 8, making inlet integration even more difficult.

Since no sideslip is considered in the calculations, only one half of the forebody has to be meshed. The Hyper X mesh requires for example 770 000 nodes (figure 6). The forebodies derived from the reference configuration have been calculated with a 500 000 node grid. In order to have a more coherent set of calculations, ONERA computed the waverider forebody as well, using a 360 000 node grid given by DLR.

Turbulence is modelled by the algebraic Baldwin-Lomax model and turbulent flow is assumed from the nose tip.

Reference forebody calculations and modified shapes calculations were performed on previous ONERA CRAY C90 computer, solving the Reynolds Averaged Navier-Stokes equations with version 5 of FLU3M code [9]. Those calculations were rather time consuming (more than 40 h CPU each) since 8000 iterations in the implicit phase were required to get a converged solution. Hyper X and DLR waverider forebodies calculations were performed more recently on ONERA SX-4 computer with an optimised version of FLU3M code using LU factorisation [10]. In the Hyper X case, only 1500 iterations were necessary to reach convergence, needing 4000 s CPU.

#### 3D analysis

Examples of 3D Mach number distributions are given on figure 7. The shock detachment from the bottom surface is clearly more important with blunted shapes and even more when there is in addition nose spatula effect (Mod 1), which can be explained by an increase in pressure recovery losses. Indeed, blunted noses create an entropy layer due to the strong shock curvature.

The waverider forebody seemingly produces an almost two-dimensional shock at bottom side, which is certainly due to the concave cross section shape; the edges act as sidewalls, preventing from mass flow spillage. In the Hyper X configuration, the shock remains quite two-dimensional in the upstream part, while the span is close to the leading edge width. More downstream, three-dimensional effects become very important and lead to a strong shock curvature in spanwise direction.

A close examination of the flow fields around the different forebody shapes shows that inlet integration above the front shock is possible in all cases within a 4.2m distance from the nose tip. The inlet entry conditions and precompression effects are therefore compared for such a forebody length. On the average, a 3.5 meter long forebody is enough to insure inlet integration at Mach 8, incidence  $+2^\circ$ . Narrow nose forebodies like waverider and Mod 2 configurations can however be distinguished, both needing 4.2 m for inlet integration, as well as Mod 1 (spatula shaped blunted nose) and Mod 6 (gradual windward compression) configurations allowing an upstream inlet integration (less than 3 m required).

### Inlet entry conditions

Next table compares the integrated mass flow (and stream tube area ratio) through the projected front area of the entire inlet (capture area  $A_1 = 0.32 \text{ m}^2$ ) as well as the average Mach number and pressure recovery of the flow field entering the inlet.

Forebody	$\epsilon_{\infty 0}$	Mass flow (kg/s)	$M_0$	$\eta_{\infty 0}$
REF	1.678	35.838	5.809	0.408
Mod 1	1.373	29.318	5.393	0.245
Mod 2	1.833	39.150	6.008	0.515
Mod 3	1.849	39.488	5.968	0.504
Mod 4	1.694	36.174	5.758	0.397
Mod 5	1.698	36.250	5.907	0.443
Mod 6	1.610	34.378	5.703	0.362
Hyper X	1.742	37.210	6.254	0.582
Waverider	2.099	44.832	6.109	0.634

Table 2 : Inlet integration at 4.2 m ( $A_1 = 0.32 \text{ m}^2$ )

This table clearly indicates that the waverider achieves the best compression process. Indeed, the amount of mass flow captured by the inlet is at least 13.5 % larger with the waverider than with the other configurations. Blunt nose forebodies achieve the poorest compression process (see reference forebody and modified shapes 1, 5 and 6). In addition, as already noticed from 3D views, nose spatula effect (Mod 1 and Mod 4) is not suitable as far as nose bluntness does not become negligible like in Hyper X configuration for instance. However, in this latter case, while the flow field entering the inlet exhibits a quite high pressure recovery, the compression process remains inefficient because the flow is spilled sideways. Pressure recovery distributions in the entry plane of the inlet are compared on figure 8.

The lower surface curvature of Mod 6 forebody being gradually increased backwards, it leads to a vertical pressure gradient inside the shock layer and consequently at the inlet face. Indeed, the strongest pressure waves stemming from the aft part of the lower surface have still not propagated through the inlet at station  $X = 4.2 \text{ m}$ .

The assessment of the boundary layer thickness at the inlet face is not straightforward. The problem lies in the fact that the inviscid reference conditions cannot be readily chosen. The boundary layer notion is indeed less clear than in academic flow fields like flat plate or conical flow fields because of the entropy layer due to the nose bluntness. A preliminary look at the velocity profiles is necessary to define a reference inviscid velocity. Whatever the method chosen for the boundary

layer thickness assessment, the forebody configurations providing the inlet with a large mass flow are unsurprisingly those for which the boundary layer is thin. The Hyper X forebody can be set apart, as mass flow losses are mainly due to edge effects and not to viscous losses (see above).

### Aerodynamic coefficients

Comparisons in axial and normal force coefficients, lift-to-drag ratio and centre of pressure distributions are given on figure 9 as well as comparisons in geometric coefficients like the cross section area and the volume. All coefficients are given for the entire forebody.

Friction contribution amounts to only 20 % of the global axial force resultant because of compressibility effects in high speed flows. Friction contribution to the normal force is negligible.

Again, the waverider appears to be outstandingly more efficient than the other forebodies because of its sharp nose and smaller cross section. On the other hand it offers less volume for fuel and system integration.

In spite of its small bluntness, the nose drag of the Hyper X is not negligible, which is due to its strong spatula effect. As a general rule, the nose drag amounts to a significant percentage of the overall drag, except in the waverider case for which the nose bluntness is negligible. Considering a 4.2 meter long forebody, the ratio of nose drag to overall drag lies around 50% in blunt nose configurations and exceeds 60% in Mod 1 configuration (blunt spatula shaped nose).

For a 4.2 m long forebody, the centre of pressure is located between 2.3 m and 3.2 m from the nose tip depending on the configuration chosen. The lower surface camber of Mod 6 forebody results in a downstream location of the centre of pressure.

### Parametric study synthesis

The nose has to be carefully designed to avoid excess drag since, unless very sharp, it is a major contributor to the overall drag. Blunted and spatula shaped noses must be rejected since they result in an increase in drag. In addition, spatula effect do not improve the uniformity and two-dimensionality of the flow field delivered to the inlet. Blunted noses produce a shock rather distant from the lower surface of the forebody, but they are also associated with higher pressure recovery losses and thicker boundary layers.

The introduction of lower surface camber does not seem favourable because of the heterogeneous flow field generated at the inlet face.

The waverider achieves the best compression process because it leads to a very uniform flow field at the inlet face and provides the inlet with a large mass flow. In this configuration, the concave edges prevent from excess mass flow spillage. However, this forebody has the drawback to offer less volume than the others for fuel and system integration. The Hyper X forebody does not perform satisfactorily because of 3D effects generated by its bottom side design.

### Inlet studies

Preliminary propulsion performance calculations showed that the mass flow was the governing parameter for the propulsion efficiency of a DMR engine. That is why ONERA focused on internal compression inlets in order to avoid excess spillage, especially at low Mach numbers.

The inlet design is constrained by the combustion chamber design and by the DMR operation. At Mach 4, the inlet works classically, namely the strong shock is located near the engine entrance, at the inlet throat. At higher Mach numbers, the flow is fully supersonic inside the inlet and a supersonic jet enters the engine.

The inlet has to achieve an efficient compression process between Mach 4 and Mach 8. The amount of compression must be high enough inasmuch as the inlet is operated with a fixed geometry. Indeed, at high Mach numbers, the inlet has to slow down sufficiently the supersonic air flow otherwise supersonic combustion becomes less efficient due to fuel mixing problems and combustion delays. At Mach 4, the terminal shock must be as weak as possible in order to minimise pressure recovery losses while keeping enough margin with respect to the unstart limit. On the other hand, there is no strong constraint associated with self-starting of the inlet at low Mach number because of the type of mission chosen (decelerating trajectory from Mach 8 to Mach 4).

Based on previous works conducted at ONERA [11], an internal inlet was designed for the purpose of JAPHAR project and a scale 0.4 model was built for experiments in S3MA wind tunnel. A sketch of the inlet is given figure 10.

The main features of this concept are the two boundary layer bleed levels. The upstream bleed system is located downstream the first compression ramps (the

cowl and the two compression ramps at fuselage side) and the second one is located between the small internal compression ramps and the engine entrance. Whereas downstream bleeds are supposed to stabilise the strong recompression shock at low Mach numbers, the upstream bleeds are expected to prevent from strong shock-boundary layer interactions, but not really to bleed mass flow efficiently since the air flow is always supersonic at this level.

The inlet throat is close to the inlet section of the combustion chamber, the upstream part of which being the inlet diffuser. This is a very strong constraint for the inlet inasmuch as the struts are likely to induce pressure recovery losses and unstart problems. The height to width ratio at the inlet throat is  $\frac{1}{4}$ .

A few 3D Navier-Stokes calculations of the isolated inlet were performed before the test campaigns in order to assess 3D and viscous effects and more particularly to verify whether large separations due to shock-boundary layer interactions were likely to occur or not. A Mach number 5.5 calculation is presented figure 11 for half an inlet configuration.

A first test campaign was conducted in April 1998 in S3MA wind tunnel in order to assess the performance of the isolated inlet between Mach number 3 and 5.5.

In order to avoid starting problems, very likely to happen due to the internal compression, the cowl was driven by a hydraulic jack. Indeed, at the beginning of a run, the cowl was positioned in such a way that the inlet contraction ratio allowed self-starting. Then once the inlet was started, the cowl was quickly driven to the desired position. Despite this device, it was however impossible to start the inlet at Mach number 3, very likely because of numerous shock-boundary layer interactions. However, Mach number 3 corresponds to the Mach number of the flow precompressed by the forebody; hence this Mach number does not really fall within the range of interest for JAPHAR flight test vehicle.

The inlet model can be seen mounted in S3MA half nozzle on figure 12 together with the hydraulic jack. The model was connected to a mass flow meter and a rotating butterfly valve allowed to throttle the inlet. The characteristic operating curves of the inlet could thus be obtained. Pressure taps were distributed along the ramps and the inlet and diffuser sidewalls.

A five hole probe rake could be positioned instead of the first injection struts level in order to analyse the flow conditions at the engine face. In addition, small

windows were installed in the sidewalls in order to allow Schlieren visualisations of the internal flow field. This was particularly helpful for the understanding of the complex shock wave patterns in the vicinity of the inlet throat (see example on figure 13).

This highly modular model allowed a great number of cowl and ramps combinations to be tested. An inlet configuration was finally selected which performed satisfactorily between Mach 3.5 and 5.5 with fixed geometry (CR = 4). The maximum pressure recovery is plotted against test Mach number on figure 14. The stream tube area ratio (ratio of mass flow entering the engine to maximum mass flow value) is almost constant because of the fixed geometry nature of the inlet. The only small differences come from spillage and bleeding.

A second test campaign was conducted in December 1998 in order to take into account an incoming boundary layer. For this purpose, the inlet was installed on the floor of S3MA half nozzle so that the inlet could ingest the wind tunnel boundary layer.

The wind tunnel boundary layer was not really representative of the forebody one, which led to starting difficulties, especially at low Mach number. On the average, the maximum pressure recovery was decreased by 30 % above Mach number 3.8.

#### Nozzle / Afterbody studies

Both ONERA and DLR had a good background on SERN type nozzles [12]. Then it seemed reasonable to choose such a concept for a good integration of the nozzle to the airframe. Classical symmetrical nozzles are certainly more interesting from a performance point of view but they are likely to increase dramatically the mass budget.

A preliminary study, based on 2D Euler calculations, was conducted at ONERA in order to define a first satisfying shape. The flap length and deflection were optimised at Mach number 6 as well as the upper wall profile.

The main design constraint was a fixed geometry. The other design constraints were the available length and height for the nozzle integration to the airframe (respectively 3m and 1.3m). In addition, the engine axis was not tilted away from the vehicle axis.

The best configuration has a one meter long flap deflected 5° downward. The performance of this nozzle configuration are given in the table hereafter as a function of free stream Mach number. The axial thrust

(T) is expressed as a fraction of the ideal 1D thrust, namely the thrust which could be obtained with an ideal expansion process to the ambient pressure. The orientation of the thrust vector relative to the vehicle axis is also given.

One can see that the SERN nozzle concept performs well. Indeed, with only a small exit height (1.3 m), the selected nozzle provides 84% of the ideal axial thrust at Mach 6 (design point) whereas the required exit height in the ideal case exceeds 3m. In addition thrust vector deflection stays within acceptable limits during the vehicle flight.

MACH	4	5	6	7	8
$T / T_{1D}$	0.93	0.88	0.84	0.79	0.72
$\alpha_T$ (°)	- 10.0	+ 6.4	+ 10.1	+ 8.2	- 2.8

Table 4 : nozzle performance

Based on this preliminary design, a parametric study has been launched, relying on 3D Euler calculations. The objective is to assess 3D effects due to side spillage of the propulsive flow. The major parameter of this study are therefore the sidewalls length and shape. Another parameter under investigation is the upper wall design, including vault effect. Figure 15 gives an example of calculation performed at flight Mach number 6 with a vaulted upper wall.

At this stage of JAPHAR project a lot of work is still needed for the design of the nozzle. Viscous effects must be taken into account, with realistic inlet conditions from DMR chamber calculation. Another major problem is to assess the sudden changes in thrust vector orientation when combustion is stopped, in order to help controlling the vehicle attitude.

#### Conclusion

The aerodynamic component studies conducted in the frame of JAPHAR project for the design of an integrated propulsion system are presented in this paper. The emphasis is put on the forebody design which is a key point for an hypersonic airbreathing vehicle.

A waverider forebody proved to be the best performer among more blunted configurations and a Hyper-X like forebody and was therefore selected. Inlet studies have been mostly experimental at this stage of

the project. A fixed geometry internal compression inlet was successfully tested at S3MA wind-tunnel, between Mach 3.5 and 5.5. It proved to be a valuable candidate for dual mode ramjet applications. Further work is needed on the nozzle topic; current studies are based on SERN type concepts and require extensive use of calculations.

An integrated design process is currently undertaken in order to provide the system studies with more accurate data during the second design iteration of JAPHAR vehicle.

### References

- [1] F. FALEMPIN  
*PREPHA program. System studies synthesis.*  
XIII ISABE Congress - Chattanooga
- [2] Ph. NOVELLI, W. KOSCHEL  
*JAPHAR : A Joint ONERA-DLR Research Project on High Speed Airbreathing Propulsion.*  
XIV ISABE Congress - Paper IS - 093, Florence, 1999.
- [3] Th. EGGERS, Ph. NOVELLI  
*Design Studies for the Development of a Dual Mode Ramjet Flight Test Vehicle.*  
German Aerospace Congress 1999 / DGLR-Jahrestagung 1999, Fachsitzung :  
RHS Technologieerprobung, 27-30 September 1999, Berlin
- [4] D. SCHERRER, M. BOUCHEZ  
*Combustor Design and Injector Devices.*  
AGARD Symposium April 1997  
"Hypersonic Sustained Flight"
- [5] Th. EGGERS  
*Aerodynamischer Entwurf von Wellenreiter-Konfigurationen für Hyperschallflugzeuge.*  
DLR-FB 1999-10, Dissertation TU Braunschweig (1999).
- [6] Th. EGGERS, D. STROHMEYER  
*Design of High L/D Vehicles Based on Hypersonic Waveriders.*  
AGARD CP-600 (1997), Vol. 3, C18-1 to C18-10.
- [7] T. M. BERENS, N. C. BISSINGER  
*Forebody Precompression Effects and Inlet Entry Conditions for Hypersonic Vehicles.*  
Journal of Spacecraft and Rockets. Vol. 35, N° 1, January-February 1998.
- [8] R. VOLAND, K. ROCK, G. DISKIN, C. Mc CLINTON  
*Hyper-X Engine Design and Ground Test Program.*  
AIAA-98-1532 (Norfolk 8<sup>th</sup> AIAA Space Planes and Hypersonic Systems and Technologies Conference).
- [9] L. CAMBIER, D. DARRACQ, M. GAZAIX, Ph. GUILLEN, Ch. JOUET, L. LE TOULLEC  
*Améliorations récentes du code de calcul d'écoulements compressibles FLU3M.*  
AGARD Séville, 2 au 5 octobre 1995.
- [10] M. PECHIER, Ph. GUILLEN, R. CAYZAC  
*A Combined Theoretical-Experimental Investigation of Magnus Effect*  
AIAA Summer Conferences. 16<sup>th</sup> Applied Aerodynamics Conference. Albuquerque (USA), June 15-18, 1998.
- [11] F. FALEMPIN, Ph. DUVEAU  
*Prises d'Air à Section de Captation Variable. Application aux Lanceurs Aerobies.*  
AGARD Symposium - Fort Worth, October 1991.
- [12] P. ROSTAND, A. DUFOUR, R. HALLARD, O. PENANHOAT  
*Afterbody Testing and Comparison to CFD Simulations.*  
AIAA Paper 98-1596.



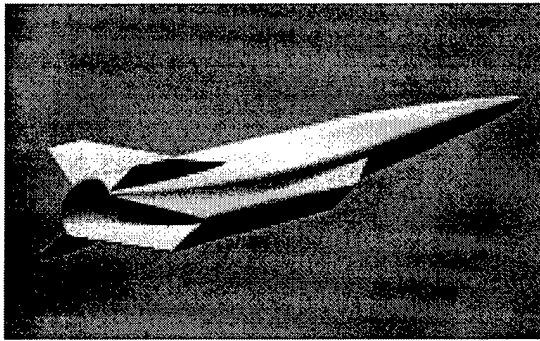


Figure 1 : Artist view of JAPHAR vehicle

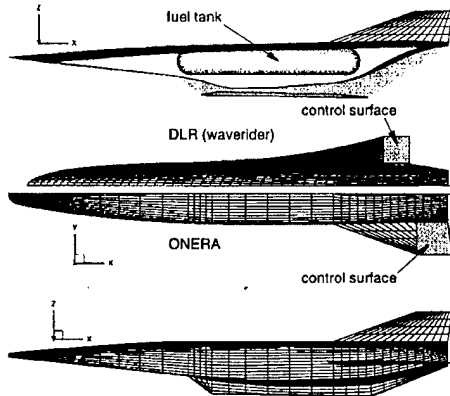


Figure 2 : Two candidate vehicles

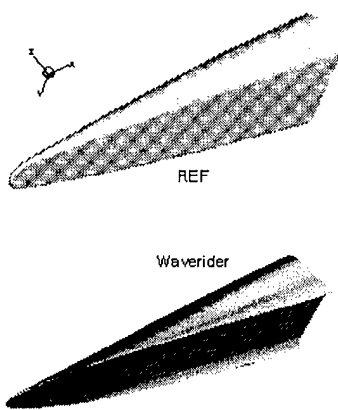


Figure 3 : Reference and waverider forebodies

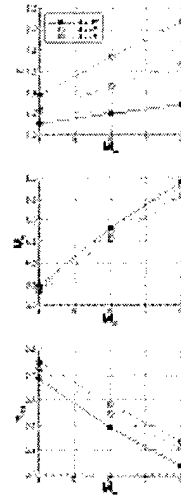


Figure 4 : Reference forebody model

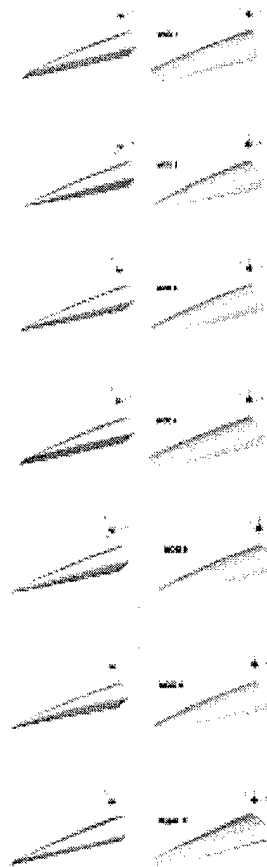


Figure 5 : Forebody shapes investigated

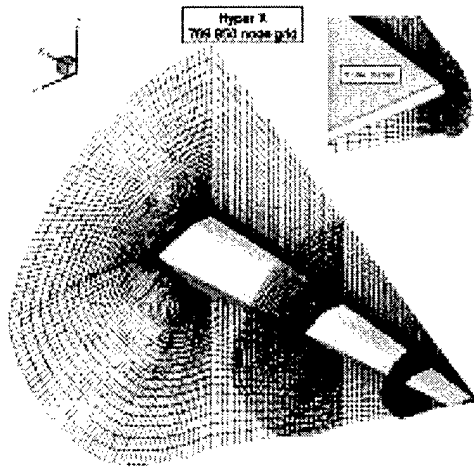


Figure 6 : Hyper-X mesh

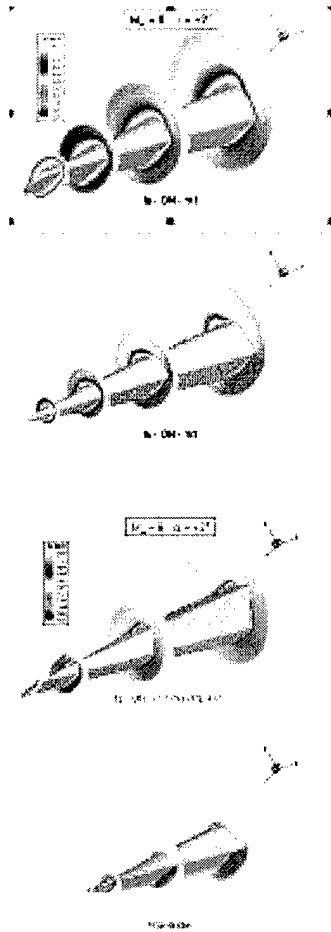


Figure 7 :  $M = 8, \alpha = +2^\circ$ , NS calculations

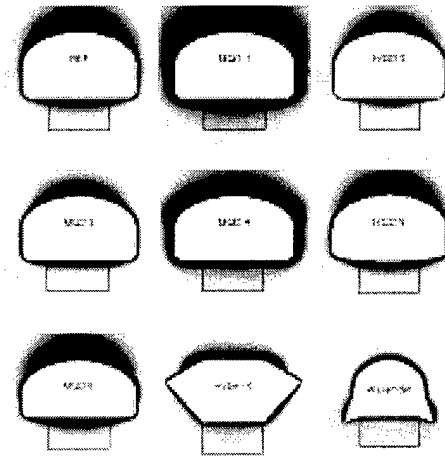


Figure 8 : Pressure recovery in the inlet entry plane

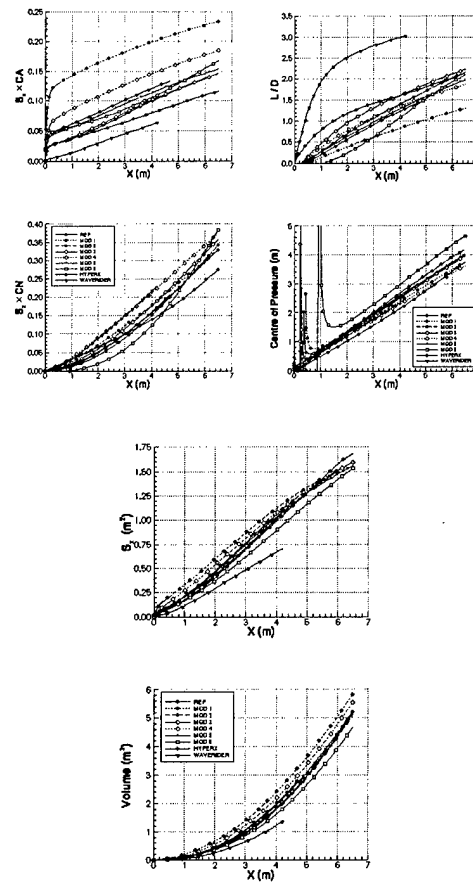


Figure 9 : Aerodynamic and geometric coefficients

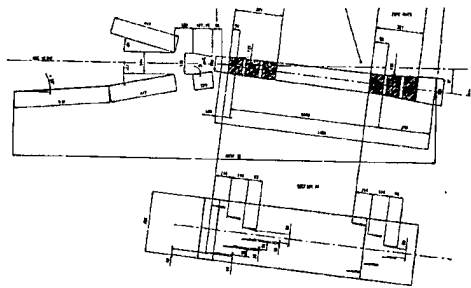


Figure 10 : Sketch of the inlet model



Figure 13 : Schlieren visualisation at Mach 5.5

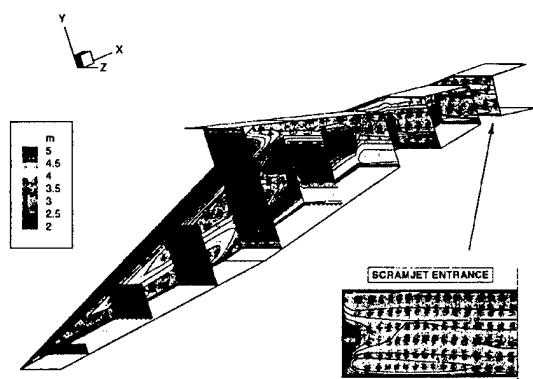


Figure 11 : Inlet 3D NS calculation at Mach 5.5

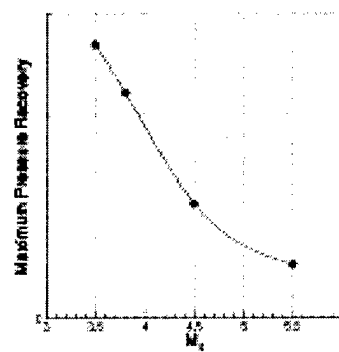


Figure 14 : Maximum pressure recovery

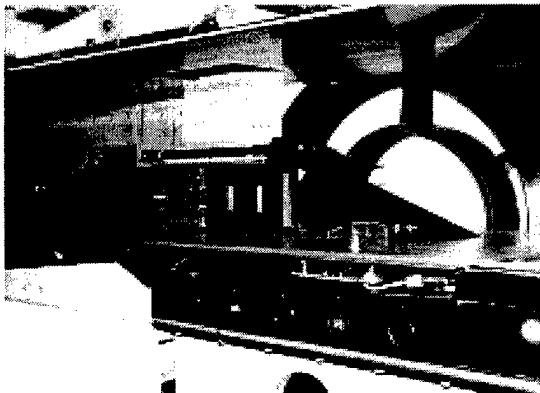


Figure 12 : Inlet model mounted in S3MA half nozzle

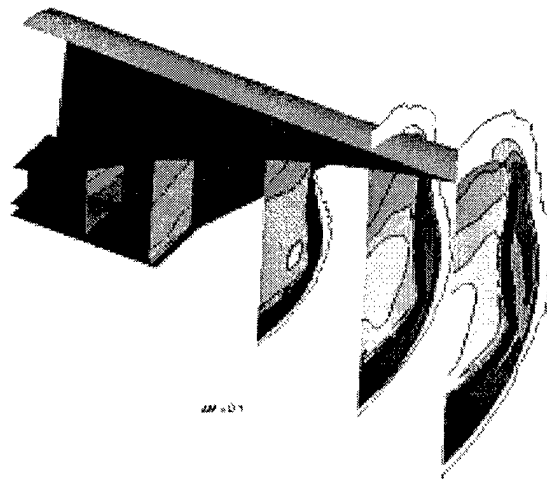


Figure 15 : 3D Euler nozzle calculation (vaulted upper wall)